Printed in the Republic of Korea
ANALYTICAL SCIENCE & TECHNOLOGY
Vol. 34 No. 4, 143-152, 2021
https://doi.org/10.5806/AST.2021.34.4.143

Enantioselective electrophoretic behavior of lipoic acid in single and dual cyclodextrin systems

Thi-Anh-Tuyet Le[1], Bao-Tan Nguyen[1], Thanh Dung Phan[2], Jong-Seong Kang[3], and Kyeong Ho Kim[1,★]

[1]*College of Pharmacy, Kangwon National University, Chuncheon 24341, Korea*
[2]*Faculty of Pharmacy, University of Medicine and Pharmacy, Ho Chi Minh City, Vietnam*
[3]*College of Pharmacy, Chungnam National University, Korea*
(Received May 14, 2021; Revised May 31, 2021; Accepted June 1, 2021)

Abstract: Capillary electrophoresis (CE) is an effective technique to study chiral recognition because it offers flexibility in adjusting vital factors. Currently, various available cyclodextrins (CDs) can be employed for the chiral separation of numerous analytes. Herein, we investigate the enantioseparation behavior of lipoic acid enantiomers in various types of single and dual CD systems through CE. Additionally, several impacted CE parameters were optimized through the systematic investigation based on the design of experiment (DoE) concept for a single system comprising a heptakis (2,3,6-tri-*O*-methyl)-β-CD and a dual system containing the combination of the single CD with a sulfated-β-CD. Consequently, absolute enantioresolution was obtained within 15 min on a common standard bare fused-silica capillary (64.5/56 cm in total/effective length, 50/365 μm inner/outer diameter), maintained at 15 °C and at an applied voltage of 24 kV. The optimal background electrolyte consisted of 6 mM heptakis (2,3,6-tri-*O*-methyl)-β-CD dissolved in the solution of 58 mM borate buffer at pH 10. Furthermore, the results of apparent binding constant experiments indicated that the *S*-enantiomer-heptakis (2,3,6-tri-*O*-methyl)-β-CD complex exhibited a stronger affinity than its *R*-enantiomer counterpart. The obtained electrophoretic mobility values could be utilized to interpret the resolution achieved at various CD concentrations and the mobility behavior of the complexes elucidated the migration order of the enantiomers in an electropherogram.

Key words: lipoic acid enantiomers, chiral separation, capillary electrophoresis, DoE, apparent binding constant

1. Introduction

Alpha lipoic acid (ALA), chemically known as 5-[(3*RS*)-1,2-dithiolan-3-yl]pentanoic acid, is a natural acid that functions as an antioxidant. It is an essential cofactor in various mitochondrial multienzyme complexes and can directly or indirectly scavenge free radicals such as the relevant reactive oxygen species or reactive nitrogen species.[1-4] Furthermore, ALA plays an important role in antioxidant defense and is effective for treating several diseases including diabetes, neuropathy, central nervous system-related

★ Corresponding author
Phone : +82-(0)33-250-6918 Fax : +82-(0)33-259-5631
E-mail : kyeong@kangwon.ac.kr

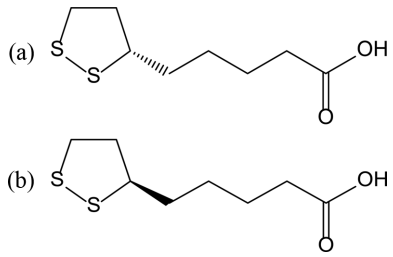

Fig. 1. Chemical structure of alpha-lipoic acid enantiomers. (a) *S*-ALA, (b) *R*-ALA

diseases, inflammation, multiple sclerosis, and obesity.[5] Recent literature suggests that ALA can strengthen body defense against SARS-CoV-2 and has proven beneficial to critically ill COVID-19 patients.[6]

The structure of ALA (*Fig*. 1) comprises an asymmetric carbon, which results in the occurrence of two enantiomeric forms of ALA. *R*-ALA is the naturally and biologically active enantiomer with higher bioavailability, potency, and therapeutic efficiency and a lower toxicological profile than *S*-ALA.[7,8] Therefore, an extensive study on the development of an analytical method for the chiral separation of ALA would be advantageous.

Currently, the ALA monograph in USP43, EP 10, BP2017, JP17, and KP XII does not include an enantiomeric test. However, enantioseparation methods based on the use of different analytical techniques such as capillary electrophoresis (CE),[9] liquid chromatography–tandem mass spectrometry (LC-MS/MS),[10-12] and high performance liquid chromatography have been investigated.[13,14] Among them, chiral separation through CE has several advantages including high peak efficiency, high resolution, fast separation, and fast screening as well as flexibility in parameter adjustment, cost-effectiveness, and environment-friendliness. However, S. Kodama *et al*.[9] demonstrated the shortcomings of CE toward the chiral separation of ALA, such as insufficient resolution (R_s) between *S*-ALA and *R*-ALA (~1.2) and the requirement of a special type of capillary (sulfonated coated capillary); they also highlighted a lack of information about the effect of some cyclodextrins (CDs) on chiral separation. The heterogeneity of chiral selector CD significantly influences their enantioseparation. In fact, the background electrolyte (BGE) comprising one CD (single CD system) or two CDs (dual CD system) can lead to the different behavior. Nevertheless, the investigation of the effect of single and the dual CD system on enantioseparation is challenging.

Additionally, the developed CE method by S. Kodama *et al.* is based on a traditional approach (one-factor-at-a-time (OFAT) approach), which is time-consuming, tedious, and costly and ignores the interactions among several vital factors. Employing the design of experiment (DoE) concept using mathematical models could solve the limitations of the OFAT approach because it facilitates systematic variation of experimental parameters and analysis of the results through a multivariate statistical technique. Consequently, it minimizes the number of experiments and provides valuable scientific information about the interactions among factors, thus resolving the unpredictable errors of the OFAT approach.[15] DoE has been extensively applied to a variety of scientific fields and specifically in the development of analytical methods because of its diverse design and statistical power.[14,16,17]

The versatility of CE is further demonstrated by its potential to determine the apparent binding constants of analyte–CD complexes. Furthermore, complexation constant values determined through CE provide a better understanding of the migration behavior, separation mechanism, and molecular interactions.

Herein, we report the enantioselective behavior of lipoic acid in a single or dual CD system by employing an innovative CE condition based on the application of the DoE concept to efficiently separate *S*-ALA and *R*-ALA on a common capillary within a short analysis time. Furthermore, different migration behaviors of each enantiomeric inclusion complex were investigated by determining apparent binding constants using the linear plotting method.

2. Experimental

2.1. Chemicals and reagents

S-ALA and *R*-ALA standards were supplied by Sigma-Aldrich (Saint Louis, MO, USA). *R*-α-lipoic

tromethamine was manufactured by Korea Biochem Pharm. Inc. The surveyed β-CDs including β-CD, 2-hydroxypropyl-β-CD (HP-β-CD), methyl-β-CD (M-β-CD), acetyl-β-CD (A-β-CD), heptakis(2,3,6-tri-*O*-methyl)-β-CD (TM-β-CD) and sulfated-β-CD (S-β-CD) were purchased from Sigma-Aldrich (Saint Louis, MO, USA). α-CD, 2-hydroxypropyl-α-CD (HP-α-CD), γ-CD and 2-hydroxypropyl-γ-CD (HP-γ-CD) were obtained from TCI (Tokyo, Japan). Carboxymethyl-β-CD (CM-β-CD) and sulfobutyl ether-β-CD (SBE-β-CD) were obtained from Wacker (Munich, Germany) and Cydex (La Jolla, CA, USA), respectively. Other chemicals and reagents were of analytical grade.

2.2. Instruments

Electrophoretic experiments were performed using a HP^{3D} CE system (Hewlett-Packard, Waldbronn, Germany) and the HP^{3D} CE ChemStation (Rev.A.06.03 (509)) software was used for instrument control and data acquisition. In all experiments, an uncoated fused-silica capillary (Agilent Technologies, Waldbronn, Germany) having a total length of 64.5 cm, an effective length of 56 cm, an inner diameter of 50 μm, and an outer diameter of 365 μm was used. The pH adjustment was monitored using a Seven Easy pH meter instruments (Mettler Toledo, Columbus, OH, USA). Design Expert software version 11 (Stat-Ease Inc., USA) was applied for experimental design and data analysis.

2.3. Sample preparation

S-ALA and *R*-ALA stock standard solutions (2000 μg mL^{-1}) were prepared in methanol. Standard samples of *S*-ALA and *R*-ALA were prepared by diluting the stock standard solutions to 100 μg mL^{-1} and 200 μg mL^{-1}, respectively, to simultaneously identify the separation behavior and migration order in preliminary experiments. A solution of *S*-ALA and *R*-ALA (1:1, 100 μg mL^{-1} for each enantiomer) was used for the DoE and apparent binding constant experiments. A *R*-α-lipoic tromethamine salt was dissolved in methanol to produce a stock solution (equivalent to 2000 μg mL^{-1} of *R*-ALA). A spiked sample containing 100 μg mL^{-1} of each enantiomer was diluted from the *S*-ALA stock standard solution and *R*-α-lipoic tromethamine stock solution.

2.4. Method development

In the primary stage, the native CDs including α-CD, β-CD, γ-CD, and their neutral/charged derivatives were individually measured at a concentration of 10 mM in a phosphate buffer (pH 8). Subsequently, potential CDs for enantioseparation were examined over a pH range of 2-10 using various buffer solutions (50 mM phosphate, 50 mM acetate, 25 mM citrate, 50 mM borate). For the dual CD system, the potential CDs were set at a concentration 10 mM as an inherent component, with each remainder was combined with the inherent CD in a 1:1 ratio. The influence of pH (pH 5, pH 7, and pH 10) on separation efficiency was investigated for the dual CD system. The CE parameters were set at 20 kV and 20 °C, with the injection mode set at 50 mbar in 3 s and a maximum wavelength of 200 nm.

The CE condition was optimized for single and dual CD systems by conducting each step of the DoE concept (screening, response surface methodology (RSM), and confirmation) separately. The output responses were evaluated and compared to select the optimal system for the chiral separation of lipoic acid.

The apparent binding constants of the complexes of each enantiomer with the inherent CD were determined by the linear plotting method, i.e., the double reciprocal approach. Electrophoretic runs were carried out with increasing concentrations (0-20 mM) of the CD in the background electrolyte (BGE). The electrophoretic mobility (μ) of the enantiomer–CD complex was calculated from the migration time (t) to yield the apparent binding constant (K) value by using the ratio of the intercept and slope of linearity.[20]

3. Results and Discussion

3.1. Effect of single CD and dual CD system on chiral separation

3.1.1. Single CD system

ALA is a weak acid with an estimated pK_a of ~5.1 which ionizes to a lipoate monoanion in basic environments. Therefore, the initial scouting experi-

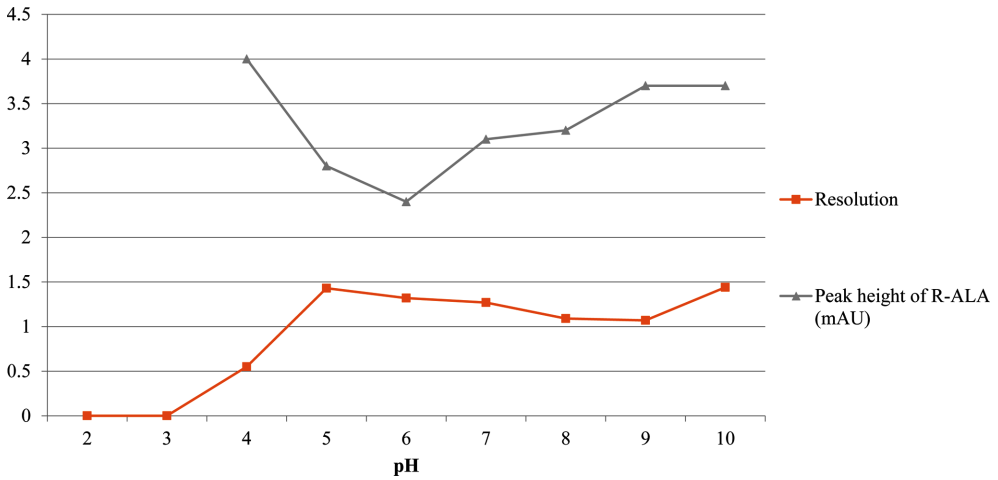

Fig. 2. The influence of pH on single TM-β-CD.

ments were carried out in a BGE containing 10 mM of CD in a solution of 50 mM sodium phosphate dibasic buffer (pH 8). Among the 12 investigated CDs, which include α-CD, β-CD, γ-CD, HP-α-CD, HP-β-CD, HP-γ-CD, A-β-CD, M-β-CD, TM-β-CD, CM-β-CD, S-β-CD, and SBE-β-CD, only the TM-β-CD led to partial enantioseparation (R_s = 1.09) and facilitated the preferred migration order (migration of *S*-ALA before *R*-ALA).

Subsequently, 50 mM sodium phosphate monobasic (pH 2, pH 3), 50 mM sodium acetate (pH 4), 25 mM sodium citrate (pH 5, pH 6), 50 mM sodium phosphate monobasic (pH 7), and 50 mM sodium tetraborate (pH 9, pH 10) were studied as alternate BGEs. As illustrated in *Fig*. 2, the signal of separation appeared at a pH of >4. In strong acidic environments, *S*-ALA and *R*-ALA could not be discriminated in a long migration time or even no peaks could be detected within 120 minute at pH 2. An improved resolution was observed when the citrate (pH 6) and borate (pH 10) buffers were used as the BGE. However, the citrate buffer produced a high current, increased the noise, and reduced the sensitivity of the main peaks.

Thus, the sodium tetraborate buffer and TM-β-CD were chosen for further experimentation.

3.1.2. Dual CD system

Conventionally, the dual CD system used for enantioseparation consists of a charged CD and a neutral or native CD. However, systems with two neutral CDs or two charged CDs occasionally show higher resolution.

Based on the scouting results in single CD system, TM-β-CD was selected as an inherent element in the dual CD system. Among the 11 investigated combinations at pH 10, six dual systems were considered to be promising. Therefore, further studies to evaluate the effect of pH on these potential combinations were performed using suitable buffers. Unlike the single CD system, the dual system containing a mixture of TM-β-CD and a negatively charged CD (CM-β-CD, S-β-CD, and SBE-β-CD) displayed a synergistic relationship in term of separation efficiency. Conversely, the separation efficiency was low when a combination of neutral CDs (HP-α-CD and HP-γ-CD) or a neutral and native CD (γ-CD) was used (*Table* 1). Although the coupling of TM-β-CD and SBE-β-CD led to the baseline separation, the challenge was to shorten the long migration times. The resolution obtained for dual CD systems containing CM-β-CD improved at pH 5.0; however, the complexes formed with the analytes were unstable in the acetate buffer. The chiral co-selector of TM-β-CD and S-β-CD enhanced the separation of *S*-ALA and *R*-ALA as it proceeded within a reasonable time. Therefore, this co-selector was considered as the representative of the dual CD

Table 1. Influence of BGE on the enantioseparation of dual CD systems

No	Investigated CDs			TM-β-CD conc. (mM)	Acetate pH 5.0		Phosphate pH 7.0		Borate pH 10.0	
	Name	Type	Conc. (mM)		Migration time (min)	Resolution	Migration time (min)	Resolution	Migration time (min)	Resolution
1	α-CD	Nature	10	10	-	-	-	-	12.229	No
2	HP-α-CD	Neutral	10	10	8.754	No	12.481 12.577	0.6	12.397 12.490	0.78
3	γ-CD	Nature	10	10	9.442 9.510	0.79	14.493 14.670	0.79	12.891 13.035	1.19
4	HP-γ-CD	Neutral	10	10	9.286 9.357	0.83	13.682 13.833	0.75	12.881 13.019	1.14
5	β-CD	Nature	10	10	-	-	-	-	12.049	No
6	HP-β-CD	Neutral	10	10	-	-	-	-	11.639	No
7	M-β-CD	Neutral	10	10	-	-	-	-	11.486	No
8	TM-β-CD	Neutral	10	0	8.821 8.903	1.05	13.922 14.152	1.32	12.904 13.085	1.43
9	A-β-CD	Neutral	10	10	-	-	-	-	11.685	No
10	SBE-β-CD	Negative	10	10	29.600 30.334	1.5	No peak within 120 min		30.753 31.462	1.5
11	CM-β-CD	Negative	10	10	16.368 16.629	1.45	32.439 33.751	0.86	19.786 20.488	1.26
12	S-β-CD	Negative	10	10	11.039 11.156	1.23	18.979 19.384	1.58	14.328 14.541	1.51

Table 2. *p*-values in ANOVA statistical parameters from screening results

Responses	Single CD system						Dual CD system					
	A-Voltage	B-Temp.	C-Inject time	D-Buffer pH	E-Buffer conc.	F-TM-β-CD conc.	A-Voltage	B-Temp.	C-Buffer pH	D-Buffer conc.	E-TM-β-CD conc.	F-S-β-CD conc.
Resolution	0.0002	<0.0001	<0.0001	<0.0001	<0.0001	0.0013	<0.0001	<0.0001	0.0017	0.0002	-	<0.0001
Migration time of *R*-ALA	<0.0001	<0.0001	0.0581	<0.0001	<0.0001	<0.0001	<0.0001	<0.0001	0.0249	<0.0001	0.0114	-
Peak height of *S*-ALA	0.6707	0.0002	<0.0001	0.0009	0.1587	0.0018	0.0001	-	0.0585	<0.0001	<0.0001	0.0022
Peak height of *R*-ALA	0.1523	<0.0001	<0.0001	<0.0001	<0.0001	0.0001	0.0019	0.0021	-	<0.0001	<0.0001	0.0036

systems for subsequent evaluations.

3.2. Optimization by DoE

3.2.1. Experimental design for a single CD system

The screening design was developed by utilizing a two-level full factorial design to identify the critical electrophoretic parameters and obtain primary knowledge space. Based on scouting experiments, the following CE parameters were studied in detail: voltage (15-30 kV), temperature (15-30 °C), injection time (3-10 s), borate buffer concentration (20-80 mM), pH (8.3-10), TM-β-CD concentration (5-15 mM). The resolution between the two enantiomers, the migration time of *R*-ALA, and the height of each main peak were selected as target responses. Six experiments of the 22 runs were set at the center point of the design to estimate its repeatability. Following the analysis of the results, the analysis of variance (ANOVA) statistical parameters were calculated for the important models which were selected from the half-normal plot and the pareto chart. As highlighted in *Table* 2, the statistical data indicate that all the chosen factors significantly affected at least two responses (p-value < 0.05), with straightforward influence patterns observed

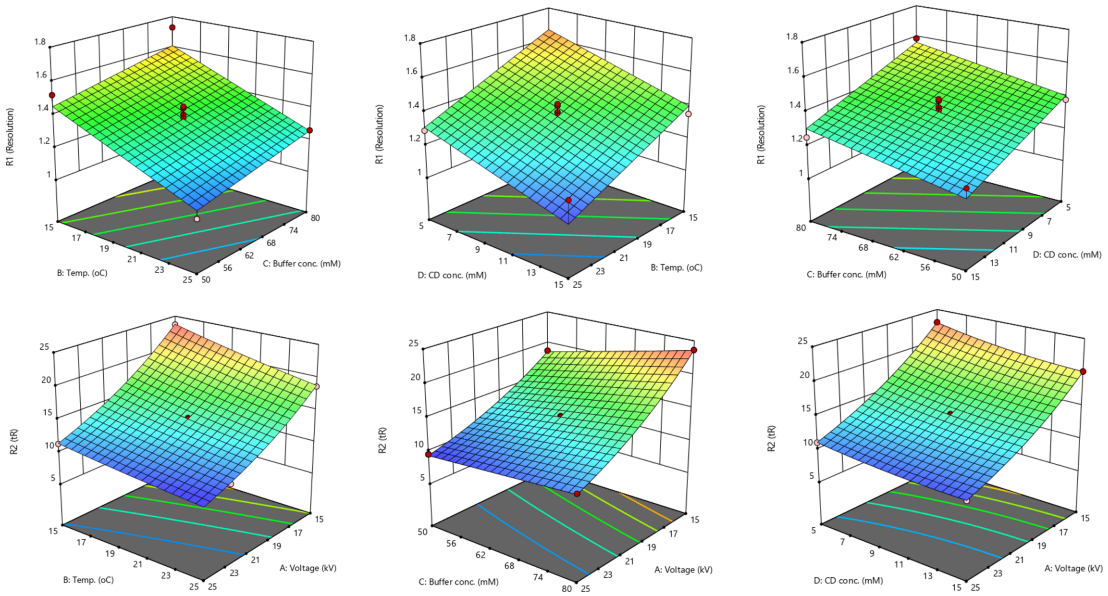

Fig. 3. 3D response surface plots of critical interactions in single CD system for resolution and migration time

for the buffer pH and injection time. For instance, higher resolutions and peak heights were obtained while using a more basic buffer. Additionally, increasing injection time contributed to higher peak heights but produced an inferior resolution. The separation efficiency was prioritized over other parameters in this study. Therefore, the pH of the borate buffer was maintained at pH 10 with the injection mode set at 50 mbar in 3 s in the subsequent stages.

The domain of the remaining parameters were narrowed (i.e., voltage, 15-25 kV; temperature, 15-25 °C; borate buffer concentration, 50-80 mM; and TM-β-CD concentration, 5-15 mM) for the RSM study because of the screening step. The Box-Behnken

Table 3. The optimization of single and dual CD system

		Single CD	Dual CD system
Factors and ranges in RSM		Voltage (15-25kV) Temperature (15-25°C) Buffer conc. (50-80mM) TM-β-CD conc. (5-15mM)	Voltage (15-25kV) Buffer conc. (50-80mM) S-β-CD conc. (5-15mM)
Responses (Goal * Importance)		Resolution (Maximize * 5) Migration time of peak *R*-ALA (Minimize and ≤15 * 3) Peak height of *S*-ALA (Maximize * 1) Peak height of *R*-ALA (Maximize * 1)	
Total number of experiments		33 runs	15 runs
Optimal CE condition	Voltage (kV)	24	22
	Temperature (°C)	15	15
	Buffer conc. (mM)	58	50
	Buffer pH	10	8.3
	TM-β-CD conc. (mM)	6	15
	S-β-CD conc. (mM)	-	6.5
	Injection mode	50 mbar in 3 seconds	

design was built comprising of 33 runs divided into three blocks. From Box–Cox plots, the migration time of *R*-ALA was underwent to square root transformation. The influence of variables and interactions between them on each response was illustrated using model graphs. Improving the resolution of CE necessitates the cooperation between various parameters such as low temperature, low concentration of TM-β-CD, and high concentration of buffer in the BGE (*Fig.* 3). Conversely, this cooperation and the use of a lower voltage led to the longer migration times and lower sensitivity of the analytes.

The optimal conditions (*Table* 3) close to the target values were selected from 81 recommended solutions on the basis of the goal and degree of importance of each response. Finally, model predictability was examined in the confirmation step to ensure that the observed values were within the prediction interval (PI low 95% and PI high 95%). Under the optimal conditions, *S*-ALA and *R*-ALA were completely separated ($R_s \approx 1.65$) and had a migration time of 12.2 and 12.4 min, respectively (*Fig.* 4).

3.2.2. Experimental designs for dual CD system

The two-level full factorial and Box-Behnken design were chosen for screening and the RSM study, respectively, for the corresponding dual CD system.

Preliminarily, six factors (voltage, 15-30 kV; temperature, 15-30 °C; borate buffer concentration, 20-80 mM; pH, 8.3-10; TM-β-CD concentration, 3-15 mM; S-β-CD concentration, 3-15 mM) were selected for screening. The list of 20 runs including four center points was carried out over 2 days. The critical factors for RSM were selected on the basis of the evaluation from the half-normal plot, pareto chart, ANOVA data and prediction models. The temperature, buffer concentration, and the TM-β-CD concentration demonstrated negligible effects on the responses (especially resolution and migration time) and were excluded for the reduced RSM design.

The Design for optimization step included 15 runs having a narrow domain for each vital variable (*Table* 3). The 3D response surface plots in *Fig.* 5 demonstrated the influence of interactions among factors on the crucial responses (resolution and migration time of *R*-ALA). The low values for the voltages and buffer concentrations contributed to an acceptable resolution. Meanwhile, the short migration time corresponded primarily to the high applied voltage. Additionally, the peak height of *S*-ALA and *R*-ALA was enhanced

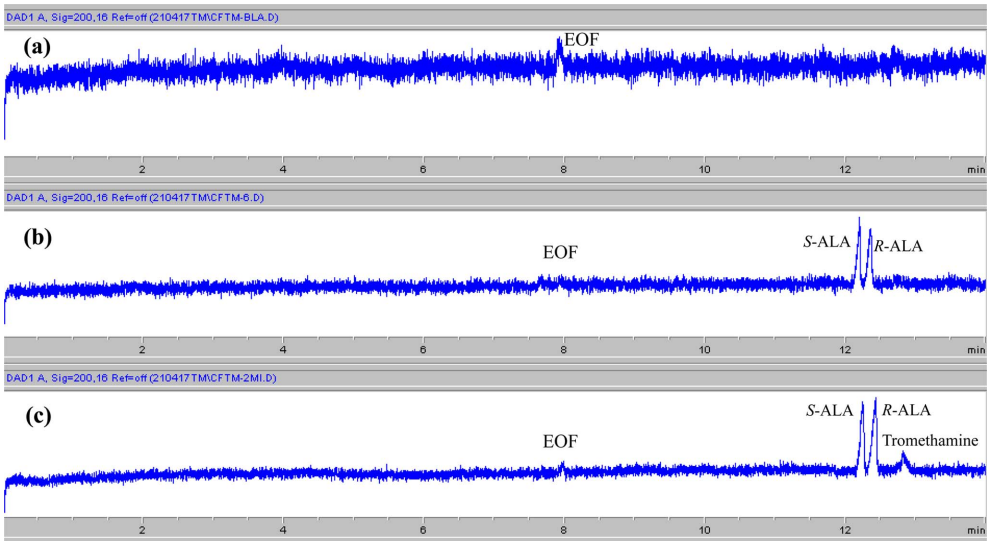

Fig. 4. Typical electropherograms of (a) Blank, (b) Standard solution, (c) Spiked *S*-ALA standard in *R*-α-lipoic tromethamine sample solution. CE condition: voltage, 24 kV; temperature, 15 °C; injection time, 50 mbar in 3s; BGE, 58 mM sodium tetraborate pH 10 containing 6 mM TM-β-CD; PDA detector, 200 nm; current, 75 μA.

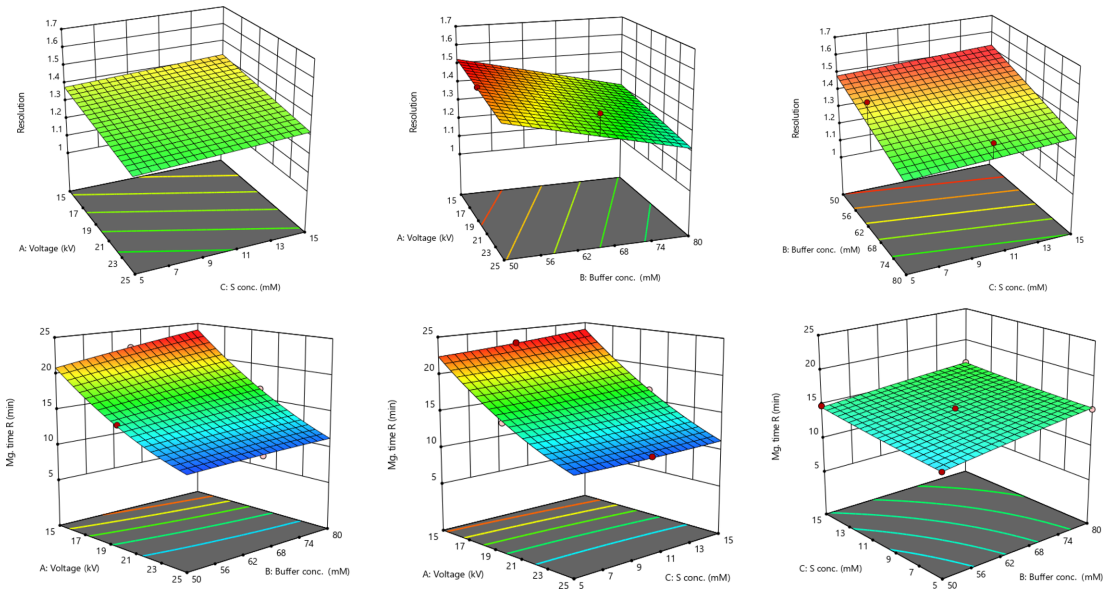

Fig. 5. 3D response surface plots of interactions in dual CD system for resolution and migration time

when a BGE with a low concentration of buffer and S-β-CD was used.

The same response criteria were set in the numerical optimization feature of the DoE software. The first condition among 88 recommendations was selected as the optimum condition for the dual CD system (*Table* 3), following which the confirmation procedure for this optimal condition was successfully performed (n = 6). *S*-ALA and *R*-ALA were separated with an R_s of ~1.37 and migrated at 11.4 and 11.5 min, respectively.

The dual CD system exhibited the same effect on the migration order but did not bestow a competitive discrimination ability as that by a single CD system.

3.3. Apparent binding constant

The apparent binding constant between the *R* and *S* enantiomers and TM-β-CD was determined on the basis of the differences in the effective electrophoretic mobility under varying CD concentrations.

Mobility (μ) was calculated based on the migration time (t) using the following equation:

$$\mu = I/tE = IL/tU$$

where *I* is the effective capillary length, *L* is the total capillary length, *U* is the applied voltage, and *E* represents the electric field.

$$\mu = \mu_i + \mu_{EOF}$$

where μ_i is the electrophoretic mobility and μ_{EOF} is the electroosmotic mobility.

However, electrophoretic mobility was essentially impacted by the viscosity of the running buffer. The high concentration of the CD resulted in a more viscous buffer solution. Therefore, Goodall *et al*. postulated the viscosity correction based on the current at [CD] = 0 and [CD] = [C]. Consequently, the corrected mobility was calculated by multiplying electrophoretic mobility with the ratio of current ($I_0/I_{[C]}$).

The apparent binding constant (K) was determined according to the following equation:

$$K[C] = \frac{\mu_f - \mu_i}{\mu_i - \mu_c}$$

where μ_f is the electrophoretic mobility of the free analyte, μ_C is the electrophoretic mobility of the complexed analyte, and μ_i is the obtained analyte mobility at the CD concentration [C].

The double reciprocal approach in the linear plotting methods describes the relationship between such

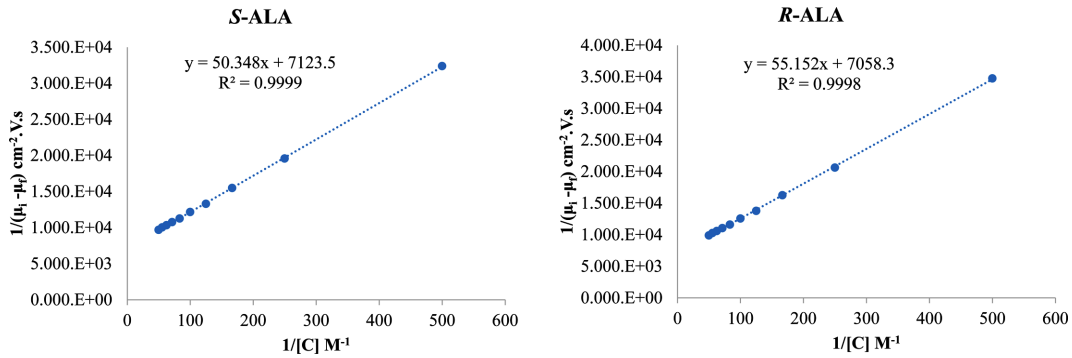

Fig. 6. Double-reciprocal plots for the complex of *S*-ALA and *R*-ALA with TM-β-CD

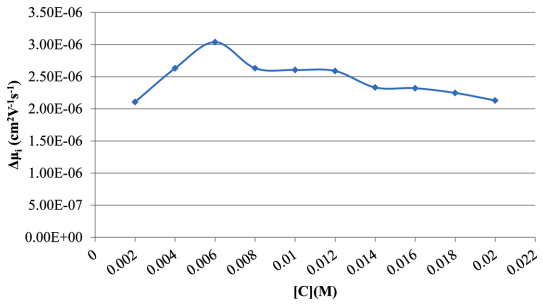

Fig. 7. Difference in effective electrophoretic mobility between *S*-ALA and *R*-ALA complex

parameters as:

$$\frac{1}{\mu_i-\mu_f}=\frac{1}{(\mu_c-\mu_f)K}\frac{1}{[C]}+\frac{1}{\mu_c-\mu_f}$$

A plot of $\frac{1}{\mu_i-\mu_f}$ against $\frac{1}{C}$ gives K (intercept/slope)

The apparent binding constants between the *S*-and *R*-enantiomer of lipoic acid with TM-β-CD calculated from the intercept and the slope of the linearity were determined to be 141 and 128 M^{-1}, respectively (*Fig.* 6). The higher apparent binding constant of the (*S*)-enantiomer–TM-β-CD complex indicated a stronger affinity of the (*S*)-enantiomer to TM-β-CD as compared to that of the (*R*)-enantiomer.

Additionally, the difference in the electrophoretic mobility between the temporarily formed complexes can explain the migration order and enantioseparation capabilities at different CD concentrations. The higher electrophoretic mobility of *S*-ALA allows for its complex to migrate before *R*-ALA. As illustrated in *Fig.* 7, the best discrimination was achieved at a TM-β-CD concentration of 6 mM, whereat $\Delta\mu_i$ was found to be the highest.

In a previous study,[21] M. Trentin *et al*. assumed the apparent binding constants of the complexes of each lipoic acid enantiomer and various CDs including TM-β-CD to be very close and indistinguishable. Conversely, the present study provides evidence contrary to their conclusion, with the comprehensible and appropriate to the practical reality.

4. Conclusions

The selection of a suitable CD is crucial for chiral separation and the investigation of host-guest interaction. Herein, the enantioselective behavior of lipoic acid was investigated by using single and dual CD systems. A reliable, fast, and effective CE-based method was developed to discriminate between the two enantiomers of lipoic acid.

The optimized method absolutely separated *S*-ALA and *R*-ALA with a favorable resolution (Rs = 1.65), using a common capillary, and within the shorter analysis time (15 minutes) than previous CE method. Furthermore, the results of the apparent binding constant experiments clearly explained the migration behavior and the robustness of each enantiomer complex as well as the chiral recognition ability of TM-β-CD over a range of concentrations.

Acknowledgements

This research did not receive any specific grant

from any public, commercial, or non-profit funding agencies. The authors would like to thank the Institute of New Drug Development and Research and the Central Laboratory of Kangwon National University for the use of their analytical equipment. We would like to thank Editage (www.editage.co.kr) for English language editing.

References

1. J. Bustamante, J. K. Lodge, L. Marcocci, H. J. Tritschler, L. Packer and B. H. Rihn, *Free Radic. Biol. Med.*, **24**(6), 1023-1039 (1998).
2. A. R. Smith, S. V. Shenvi, M. Widlansky, J. H. Suh and T. M. Hagen, *Curr. Med. Chem.*, **11**(9), 1135-1146 (2004).
3. W. Jones, X. Li, Zhi-chao Qu, L. Perriott, R. R. Whitesell and J. M. May, *Free Radical Biology and Medicine*, **33**(1), 83-93 (2002).
4. J. H. Suh, R. Moreau, S. H. Heath and T. M. Hagen, *Redox Rep.*, **10**(1), 52-60 (2005).
5. B. Salehi, Y. Berkay Yılmaz, G. Antika, T. Boyunegmez Tumer, M. Fawzi Mahomoodally, D. Lobine, M. Akram, M. Riaz, E. Capanoglu, F. Sharopov, N. Martins, W. C. Cho and J. Sharifi-Rad, *Biomolecules*, **9**(8), 356 (2019).
6. E. Cure and M. C. Cure, *Medical Hypotheses*, **143**, Article 110185 (2020).
7. M. Brufani and R. Figliola, *Acta Bio Medica*, **85**(2), 108-115 (2014).
8. E. Lucarini, E. Trallori, D. Tomassoni, F. Amenta, C. Ghelardini, A. Pacini and L. Di Cesare Mannelli, *Antioxidants*, **9**(8), 749 (2020).
9. S. Kodama, A. Taga, S. I. Aizawa, T. Kemmei, Y. Honda, K. Suzuki and A. Yamamoto, *Electrophoresis*, **33**(15), 2441-2445 (2012).
10. Y. Kobayashi, R. Ito and K. Saito, *Journal of Pharmaceutical and Biomedical Analysis*, **166**, 435-439 (2019).
11. R. Uchida, H. Okamoto, N. Ikuta, K. Terao and T. Hirota, *Int. J. Mol. Sci.*, **16**(9), 22781-22794 (2015).
12. Y. Kobayashi, K. Saito, Y. Iwasaki, R. Ito and H. Nakazawa, *Bunseki Kagaku*, **61**(2), 109-114 (2012).
13. G. Niebch, B. BüChele, J. Blome, S. Grieb, G. Brandt, P. Kampa, H. H. Raffel, M. Locher, H. O. Borbe, I. Nubert and I. Fleischhauer, *Chirality*, **9**(1), 32-36 (1997).
14. T. Le, T. Pham, X. Mai, C. Song, S. Woo, C. Jeong, S. Choi, T. D. Phan and K. H. Kim, *Analytical Science and Technology*, **33**(1), 1-10 (2020).
15. P. K. Sahu, N. R. Ramisetti, T. Cecchi, S. Swain, C. S. Patro and J. Panda, *Journal of Pharmaceutical and Biomedical Analysis*, **147**, 590-611 (2018).
16. X.-L. Mai, T.-V. Pham, T.-A.-T. Le, B.-T. Nguyen, N. V. T. Nguyen, J.-S. Kang, W. Mar and K. H. Kim, *Journal of Separation Science*, **43**(24), 4480-4487 (2020).
17. B.-T. Nguyen, T.-A.-T. Le, X.-L. Mai, T. N. V. Nguyen, T. D. Phan, J.-S. Kang and K. H. Kim, *Journal of Separation Science*, **44**, 2029-2036 (2021).
18. Y. Tanaka and S. Terabe, *Journal of Chromatography B*, **768**(1), 81-92 (2002).
19. Z. Chen and S. G. Weber, *Trends Anal. Chem.*, **27**(9), 738-748 (2008).
20. K. M. Al Azzam, B. Saad and H. Y. Aboul-Enein, *Electrophoresis*, **31**(17), 2957-2963 (2010).
21. M. Trentin, T. Carofiglio, R. Fornasier and U. Tonellato, *Electrophoresis*, **23**(24), 4117-4122 (2002).

Authors' Position

Thi-Anh-Tuyet Le : Graduate student
Bao-Tan Nguyen : Graduate student
Thanh Dung Phan : Associate Professor
Jong-Seong Kang : Professor
Kyeong Ho Kim : Professor